Orientation Change of Adsorbed Pyrazine on Roughened Rhodium Electrodes as Probed by Surface-Enhanced Raman Spectroscopy

Li Cui, Zheng Liu, Sai Duan, De-Yin Wu, Bin Ren,* and Zhong-Qun Tian

State Key Laboratory for Physical Chemistry of Solid Surfaces and Department of Chemistry, College of Chemistry and Chemical Engineering, Xiamen University, Xiamen 361005, China

Shou-Zhong Zou

Department of Chemistry and Biochemistry, Miami University, Oxford, Ohio 45056

Received: June 5, 2005; In Final Form: July 25, 2005

A surface-enhanced Raman spectroscopic (SERS) study of pyrazine adsorbed on roughened Rh electrodes was performed. Potential and concentration effects on the adsorption behavior of pyrazine were investigated. The SER spectra display four pairs of overlapping bands with the relative intensity of each pair being highly potential dependent, which has not been observed on other metals. The orientation change of the adsorbed pyrazine from the end-on to N/π bonded edge-on configuration is proposed to account for this potential-dependent relative intensity change. This hypothesis is further supported by the SERS results obtained at different pyrazine concentrations. In conjunction with the orientation effect, the interaction of Rh with hydrogen and oxygen generated at different potentials has a great influence on the adsorption configuration of pyrazine.

1. Introduction

Pyrazine is frequently used as a model molecule in surface vibrational spectroscopic studies due to its simple molecular structure and clear band assignment. The adsorption behavior of pyrazine on single crystalline Au and Ag,[1−5] polycrystalline Au and Ag,[6−10] mercury electrode,[11−13] and porous C electrode[14] has been extensively investigated by conventional electrochemical methods including cyclic voltammetry, differential capacitance techniques, and chronocoulometry,[1,2,6,13] as well as by spectroscopic methods, such as X-ray photoelectron spectroscopy (XPS), Auger electron spectroscopy (AES), low-energy electron diffraction (LEED),[3,4] inverse photoemission spectroscopy (IPS),[15] and surface-enhanced Raman spectroscopy (SERS).[5,8,9,16−20] These studies reveal that pyrazine adsorption strongly depends on the electronic and atomic structures of the substrates. For instance, on Au(111), pyrazine takes a horizontal orientation with the ring parallel to the surface at a low surface coverage and a negatively charged interface, whereas a vertical orientation with the molecular plane perpendicular to the surface was observed at a high coverage and a positively charged interface.[1] On Ag(111), only flat-lying pyrazine was observed in the whole potential range,[3,4] which was similar to pyrazine on a mercury electrode.[11−13] On a polycrystalline Ag electrode, pyrazine tends to stand up on the electrode with one of the nitrogen atoms anchoring at the surface; the tilted configuration was barely observed.[9,10]

SERS is a powerful tool in probing the adsorption and orientation of molecules on roughened electrode surfaces because of its high surface sensitivity and excellent spectral resolution.[21] Brolo et al. carried out systematic SERS studies of the adsorption of pyrazine on gold and silver electrodes under different surface coverages, surface morphologies, pyrazine concentrations, solution pHs, and applied potentials.[5,8,9,22] Otero and co-workers did careful theoretical calculations and SERS experiments on the pyrazine−silver system with the consideration of the charge-transfer mechanism in their calculations.[10,20,23,24] It should be pointed out that most of the previous SERS studies focused on noble metals such as Au andAg, except for very recent work from our group on nickel.[25,26] The SERS study of pyrazine on a nickel electrode revealed some significant differences from that on noble metals, which were explained by the considerable lowering of the symmetry of the adsorbed pyrazine as a result of a stronger interaction between pyrazine and the nickel electrode. Hence it is essential to extend the SERS of pyrazine to other transition metals to achieve a better understanding of the role of the chemical nature of metal on the adsorption behavior of pyrazine.

In recent years, Tian's group has successfully extended SERS studies to bulk transition metals. Good-quality surface-enhanced Raman spectra have been obtained from Pt, Rh, Ru, Ni, Fe, and Co over a wide potential range, and a surface enhancement ranging from 1 to 4 orders of magnitude has been confirmed on these roughened transition-metal surfaces using pyridine as a probe molecule.[21,25−35] In the present paper, potential- and concentration-dependent SERS study of pyrazine adsorbed on Rh surfaces was performed. The SER spectra show four pairs of overlapping bands with the relative intensity of each pair being highly potential dependent, which has not been observed on other metals. A potential-dependent orientation change of the adsorbed pyrazine on Rh was proposed to interpret the difference in the SERS of pyrazine on Rh and other metals.

2. Experiment

SERS measurements were performed with a confocal microscope Raman system (LabRam1 Dilor, France). The microscope objective for laser illumination and signal collection was of long working distance (8 mm) with 50× magnification. The excitation line at 632.8 nm was from an air-cooled He−Ne laser, and

* Corresponding author. Telephone: +86-592-2186532. E-mail: bren@xmu.edu.cn.

10.1021/jp052983y CCC: $30.25
Published on Web 08/27/2005

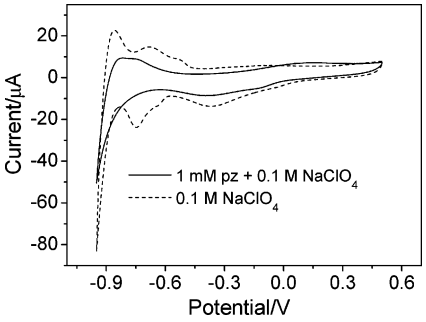

Figure 1. Cyclic voltammograms of a Rh electrode in 0.1 M $NaClO_4$ (dotted line) and 1 mM pyrazine + 0.1 M $NaClO_4$ (solid line) solution. Scan rate: 0.1 V/s.

the laser power was about 7 mW on the sample. A more detailed description of the spectroelectrochemical measurement has been given elsewhere.[34] The same electrochemical cell was used in electrochemical and SERS measurements. The detailed procedure for obtaining a high-purity Rh working electrode by zone melting of a commercially available Rh rod (99.9% purity) has been described elsewhere.[35] Before Raman and electrochemical measurements, the Rh electrode was electrochemically cleaned and roughened in 0.5 M H_2SO_4 solution with a CHI631A Electrochemical Workstation (CH Instruments, China). The electrochemical cleaning was realized by potential cycling between −0.25 and +0.8 V at a rate of 0.5 V/s until a stable cyclic voltammogram was obtained. A square-wave current with a cathodic and anodic current density of −1590 and +2640 mA/cm^2, respectively, and a frequency of 400 Hz was applied to the electrode for 2 min to roughen the electrode. Finally, the electrode was reduced at −0.2 V for 200 s, followed by the same potential cycling as the electrochemical cleaning. An XD-II Potentiostat (Xiamen University, China) was used to control the potential of the working electrode during Raman measurements. The counter electrode was a platinum wire. A saturated calomel electrode (SCE) was used as the reference electrode, and all potentials are given versus SCE. Pyrazine (99+ %, Aldrich) and $NaClO_4$ (98.0−102.0%, Alfa Aesar) were used without further purification. All solutions were prepared with Milli-Q water.

3. Results and Discussion

Figure 1 shows cyclic voltammograms of a roughened Rh electrode in 0.1 M $NaClO_4$ and 1 mM pyrazine + 0.1 M $NaClO_4$ solution. Some significant differences should be mentioned: (1) The double-layer capacitance decreases after the addition of pyrazine. (2) Oxidation of Rh commences at ca. −0.4 V in both solutions; however, the peak shifts to more positive potential in the pyrazine solution. (3) Hydrogen adsorption and desorption appear as two clear peaks at ca. −0.74 and −0.68 V in the blank solution, which is highly suppressed in the pyrazine solution. (4) Hydrogen evolution commences at a potential more negative than −0.8 V in the pyrazine solution and the cathodic current increases less rapidly with the further negative movement of the electrode potential in comparison with the blank solution, indicating the suppression of the hydrogen evolution process. Further increasing the pyrazine concentration up to 0.1 M did not lead to other obvious changes in the cyclic voltammogram except for the further suppression of the hydrogen evolution and the oxidation of rhodium. There is no indication of the electrochemical reaction of pyrazine. However, an electrochemical SERS study of the same system reveals some interesting phenomena.

Figure 2 shows selective potential-dependent SER spectra of pyrazine adsorbed on a roughened Rh electrode in 1 mM pyrazine + 0.1 M $NaClO_4$. The potential was changed stepwise from the open-circuit potential (ocp, ∼0.3 V) to −0.95 V (Figure 2a) and then returned to less negative potentials until the Raman signal of rhodium oxide was observed (Figure 2b). The spectral acquisition time was typically 20 s. The broad band at ca. 530 cm^{-1} originates from the Rh−O vibration.[36] The large bandwidth of this feature may be from various surface rhodium oxides formed spontaneously at the open-circuit potential with very close vibrational frequencies.[37,38] The band at ca. 934 cm^{-1} is due to the stretching vibration of the solution ClO_4^-. The intensity of some major bands coming from pyrazine shows a clear potential dependence, with the maximum intensity appearing at the most negative potential (−0.95 V). The band at 1650 cm^{-1} signifying the electroreduction of pyrazine was not observed, indicating the molecule is stable in the potential region used here.[9]

Most prominent in the spectra are four pairs of overlapping bands located at about 1564 and 1529 cm^{-1}, 1209 and 1232 cm^{-1}, 1008 and 1040 cm^{-1}, and 628 and 654 cm^{-1} at −0.95 V. The center positions of these bands show a mild potential dependence. Inspecting carefully the spectra, we found that the relative intensity of 1529 and 1564 cm^{-1} changes with potential and so does the pair at 1209 and 1232 cm^{-1}. To see clearly the trend of intensity change with potential, the integrated intensity of the four major bands was plotted against the potential and is shown in Figure 3. The band intensity was obtained by deconvoluting each pair of bands with the fitting program embedded in the Labspec software. It can be seen from Figure 3 that the two peaks at 1564 and 1209 cm^{-1} have nearly the same potential-dependent intensity profile; so do the other two peaks at 1529 and 1232 cm^{-1}. Regarding the other two pairs of bands at 628 and 654 cm^{-1} and 1008 and 1040 cm^{-1}, we were not able to deconvolute them unambiguously due to the

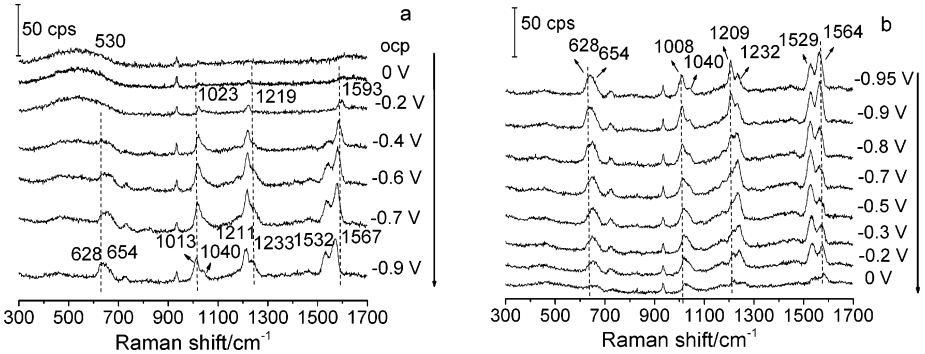

Figure 2. Potential-dependent SER spectra of pyrazine adsorbed on a roughened Rh electrode in 1 mM pyrazine + 0.1 M $NaClO_4$. (a) Potential was changed from 0 to −0.9 V. (b) Potential was changed from −0.95 to 0 V.

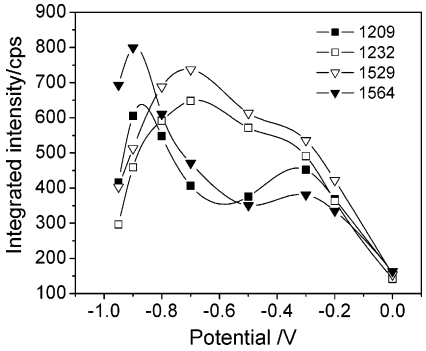

Figure 3. SERS intensity−potential profile extracted from spectra shown in Figure 2b. The integrated band intensity was obtained by deconvoluting each pair of bands.

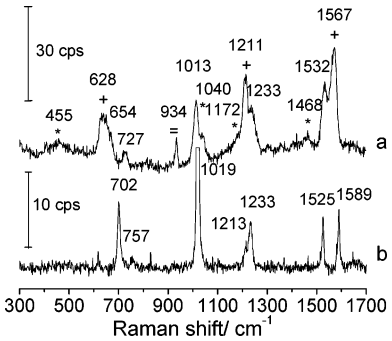

Figure 4. (a) SER spectrum of pyrazine adsorbed on a roughened Rh electrode at −0.9 V in 1 mM pyrazine + 0.1 M $NaClO_4$. (*) Raman forbidden bands (u-modes); (+) A_g modes (most enhanced); (=) perchlorate band. (b) Normal Raman spectrum of 0.8 M aqueous pyrazine solution.

significant overlapping and the low intensity. However, we can judge from the shape of the broad band that the peaks around 628 and 1008 cm^{-1} have nearly the same potential dependency as that of the 1564 cm^{-1} band, and the potential dependency at ca. 654 and 1040 cm^{-1} is nearly the same as that of the 1529 cm^{-1} band. Therefore, we can divide the above four pairs of overlapping bands into two groups according to their SERS intensity−potential profile: peak I (1564 1209, 1008, and 628 cm^{-1}) and peak II (1529, 1232, 1040, and 654 cm^{-1}). More interestingly, when the potential was moved negatively from the ocp (∼ 0.3 V) to −0.95 V, at which hydrogen evolution occurs (Figure 2a), the intensity of peak I is always higher than that of peak II. However, when the potential was moved back to potentials more positive than −0.8 V (Figure 2b), the intensity of peak II increased, while that of peak I decreased, resulting in peak II becoming even stronger than peak I. We have also performed an SERS study of pyrazine adsorption on Ag and Au and other VIIIB metals, such as Ru, Pd, Pt, Fe, and Co. The overlapping feature was not observed except for some very weak overlapping bands observed on Pt in a very narrow potential range.

To interpret the unique phenomenon observed on Rh, it is necessary to make an assignment of the vibrational bands in the SER spectra. For this purpose, we acquired the normal Raman spectrum of pyrazine from a 0.8 M aqueous solution, which was used to compare with the SER spectrum at −0.9 V. Both spectra are shown in Figure 4. In the solution spectrum (bottom spectrum), we observed a relatively strong signal for those bands of A_g mode, located at 1019 (1; ν_{ring}), 1213 (11 + 16b), 1233 (9a; δ_{C-H}), and 1589 cm^{-1} (8a; ν_{ring}); medium strong bands at 702 (6b; δ_{ring}, B_{3g}) and 1525 cm^{-1} (8b; ν_{ring}, B_{3g}); and weak bands at 757 cm^{-1} (4; τ_{ring}, B_{2g}). In the SERS spectrum

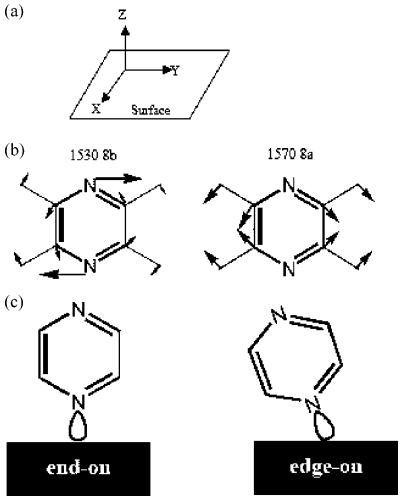

Figure 5. (a) Cartesian coordinates of pyrazine with reference to the electrode surface. (b) Schematic representation of the vibration modes of 1529 and 1564 cm^{-1}. (c) Possible orientations of adsorbed pyrazine on Rh electrode surfaces.

at −0.9 V, we could detect all the A_g modes located at 628, 1013, 1233, 1211, and 1567 cm^{-1}, corresponding to the 6a, 1, 9a, 11 + 16b, and 8a vibrations, respectively, according to literature.[9,10] Besides these A_g modes, in the SER spectrum, we also observed other bands at 455, 654, 727, 1040, 1172, 1468, and 1532 cm^{-1}, assigned to 16b (τ_{ring}, B_{3u}), 6b (δ_{ring}, B_{3g}), (4; τ_{ring}, B_{2g}), 12 (δ_{ring}, B_{1u}), 14 (ν_{ring}, B_{2u}), 19a (δ_{C-H}, B_{1u}), and 8b (ν_{ring}, B_{3g}), respectively. [9,10] The u-symmetry modes are Raman forbidden for pyrazine with D_{2h} symmetry. It is widely accepted that the appearance of forbidden bands is a result of a strong interaction of pyrazine with the substrate, which leads to lowering the symmetry from D_{2h} to C_{2V} as in the case of pyridine.[16] The forbidden band at 1040 cm^{-1} in the SER spectra has also been observed on Ni and Au;[8,25,26] however, the intensity ratio of this band to 1013 cm^{-1} is lower on Rh and Au than on Ni. It should also be pointed out that the 1525 cm^{-1} peak, which shows a medium intensity in the normal Raman spectrum, is very weak or even undetectable on Au, Cu, Ni, Fe, Co, Ru, and Pd. However, it presents as a relatively strong band on the Rh surface at 1532 cm^{-1}. This band becomes even stronger than the band at 1567 cm^{-1} when the potential was moved positively from the hydrogen evolution region.

A possible interpretation for the appearance of a strong 1529 cm^{-1} signal and the relative intensity change of the 1529 cm^{-1} band to the 1564 cm^{-1} band, specifically occurring on the Rh surface, may be the special interaction of pyrazine with Rh (adsorption orientation). For the sake of clarity in discussing the molecular orientation, the coordinates of a pyrazine molecule on the Rh surface are defined in Figure 5a. The surface is on the $X-Y$ plane and the molecular plane of pyrazine is placed on the $Y-Z$ plane when the pyrazine molecule is adsorbed with one of its nitrogen atoms pointing to the surface, with the Z-axis passing through the two N atoms. In the literature, three kinds of adsorption configuration of pyrazine on metallic surfaces have been reported: perpendicular end-on orientation with one nitrogen bound to the surface, parallel orientation with the molecular plane parallel to the surface, and in between the above.[39] The change from the perpendicular to parallel orientation should not lead to the change of the relative intensity of the 8a and 8b modes to such an extent, because both modes belong to in-plane vibration and their intensities should change synchronously. Interestingly, in the study of the pyridine system, it was found that pyridine can be adsorbed on metal surfaces in

an end-on configuration via the N atom, with the C2 axis of pyridine rotating around the adsorbed N atom on the molecular plane ($Z-Y$ plane). However, in this adsorption mode, the molecular plane can be parallel to or tilting away from the $Z-Y$ plane.[40−42] This orientation may also be possible for pyrazine on the Rh surface. Because this adsorption configuration may involve bonding via both the lone-pair electron of N atom and the π electron of the neighboring C−N bond, it may be appropriate to term this configuration a N/π bonded edge-on configuration. To determine the adsorption configuration, it is necessary to carefully analyze the vibration modes of 1529 and 1564 cm^{-1}. For this purpose, the schematic representations of them are shown in Figure 5b. The 1564 cm^{-1} band is attributed to the ring stretching mode whose polarizability changes mainly along the N−N axis of the pyrazine ring, while the 1529 cm^{-1} band is mainly attributed to the countermovement of the two N atoms leading to the change in its polarizability mainly along a direction perpendicular to the N−N axis.[9,43] According to the electromagnetic enhancement mechanism, the vibrational modes perpendicular to the surface will be most enhanced and those parallel to the surface will be least enhanced. Therefore, in the present case, if pyrazine takes the first configuration shown in Figure 5c, i.e., the end-on adsorption configuration with the N lone-pair electrons bonded to the surface perpendicularly, the 8a mode will be more enhanced than the 8b mode, which has been found in the cases of pyrazine on Au, Ag, Cu, and Ni surfaces. However, if pyrazine takes the N/π bonded edge-on adsorption configuration, this type of binding should align the molecular axis at an inclined angle along the Y direction with the 8b mode being more enhanced than the 8a mode. With this analysis in mind and recalling our experimental data, we deem that the change of the relative intensity with potential is a result of the orientation change of the adsorbed pyrazine. When the potential moves from the open-circuit potential to −0.9 V, pyrazine adopts mainly the end-on orientation, with some contribution from the N/π bonded edge-on species. However, when the potential shifts to the positive direction from the negative limit, N/π bonded edge-on adsorption becomes the dominant configuration. For the 6a and 6b modes, it is difficult to deconvolute them unambiguously due to their highly overlapped features. However, a qualitative analysis of the change of the relative intensity of 6a and 6b modes yields a similar conclusion. However, it is still difficult to explain why the intensities of mode 9a and mode 8b change synchronously as a function of potential, although their polarizabilities change in quite different directions relative to the N−N axis. Because the symmetry of the two modes is different, when charge transfer is involved in this system, a similar response to the potential may still be possible.

To further understand the origin of the relative intensity change with potential, we investigated the effect of the pyrazine concentration on the adsorption behavior of pyrazine on the Rh surface. For clarity, we present in curves a, b, and c of Figure 6 the potential-dependent integrated SERS intensity ratio of the 1529 cm^{-1} band to the 1564 cm^{-1} band (I_{8b}/I_{8a}) (other bands from peak I and peak II groups show essentially a similar trend; therefore they will not be shown here) at pyrazine concentrations of 0.001, 0.01, and 0.1 M, respectively. With this presentation, when the two bands have the same intensity, the intensity ratio will be 1. Figure 6a is extracted from the data shown in Figure 3. In 0.001 M pyrazine solution (Figure 6a), when the electrode potential changes from −0.95 V to more positive than −0.8 V, the relative intensity of the overlapping bands are completely reversed, with the 1529 cm^{-1} band being stronger than the 1564 cm^{-1} band, whereas in 0.01 M pyrazine solution (Figure 6b), the 1529 cm^{-1} band is more intense only in a narrow potential range between −0.6 and −0.4 V. In 0.1 M pyrazine solution (Figure 6c), the 1564 cm^{-1} band is always stronger than the 1529 cm^{-1} band though the difference is smaller compared to that obtained with the potential change in the opposite direction. By comparing the three intensity ratio−potential profiles in Figure 6, one can clearly see that the relative intensity of the overlapping bands is harder to change at a higher pyrazine concentration when the potential is moved to the positive direction from −0.95 V. The observation can be understood as follows: at high pyrazine concentrations, a more compact adsorption layer of pyrazine will be formed on the Rh surface, and accordingly there is less space for the pyrazine molecule to change its orientation; at low pyrazine concentrations, a less compact adlayer will be obtained and the adsorbed pyrazine can move rather freely. However, it should be pointed out that a 1 mM pyrazine solution is generally sufficient to form a monolayer adsorbate on the surface. Therefore, the dependence of adsorption behavior of pyrazine on concentration to as high as 0.1 M may indicate that the adsorption of pyrazine on the Rh surface is a kinetic rather than thermodynamic controlled process. It is interesting to note that the reorientation from bonding through the π electron of pyrazine ring to the lone electron pair of N atom on vacuum-deposited Ag has been observed when the coverage of pyrazine increases from submonolayer up to multilayer. This is revealed by the prominent spectral frequency shift and relative intensity change.[44] In contrast, in the present study in the electrochemical environment, there is no obvious frequency change at different pyrazine concentrations and all of the out-of-plane vibrations are very weak, which does not support a significant orientation change with increasing pyrazine coverage. A possible reason may be that there are always solvent, electrolyte ions, and dissociated coadsorbed species in an electrochemical system, which may be competitively adsorbed with the pyrazine molecule, leading to a different adsorption behavior of pyrazine in the electrochemical system compared with the vacuum system.

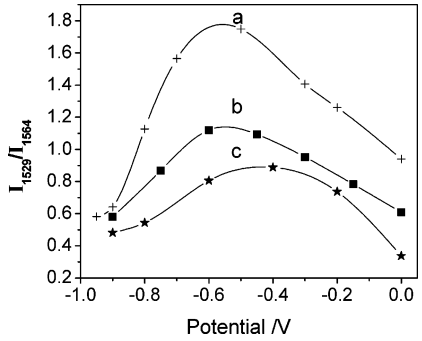

Figure 6. Potential dependence of integrated intensity ratio of the 1529 cm^{-1} band to the 1564 cm^{-1} band ($I_{1529,8b}/I_{1564,8a}$) obtained in three pyrazine solutions: (a) 1 mM; (b) 0.01 M; (c) 0.1 M.

The above presumption can explain to some extent the potential-dependent SER spectral change. However, when we examined the spectra obtained with different initial potentials, i.e., different potential change directions (from positive to negative or reverse), we found that the SER spectra showed very clear irreversibility with the potential at the time scale of spectral acquisition. This distinct irreversibility could not be explained only by the orientation change of pyrazine molecule on the Rh surface. We proposed that the interaction of Rh with hydrogen and oxygen generated at different potentials may lead to the irreversibility after we considered the strong interaction

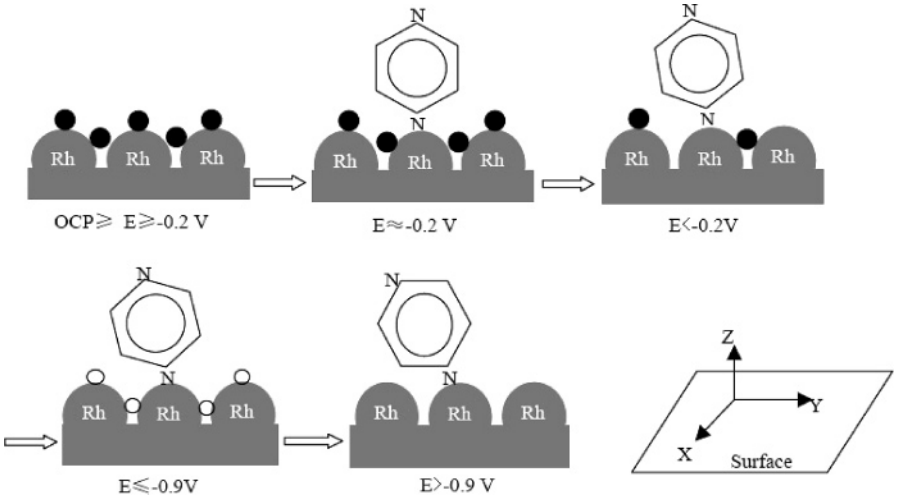

Figure 7. Schematic representation of orientation change of pyrazine on Rh surfaces with electrode potential. ●, oxygen atom; ○, hydrogen atom.

of Rh with oxygen and hydrogen. A model representing the orientation change with potential after consideration of the interaction of oxygen and hydrogen is depicted in Figure 7. A detailed discussion is given below.

It is widely accepted in electrochemical studies that there are different species on a Rh electrode at different potentials: at the open-circuit potential, the surface is dominated by the oxygen-containing species; at very negative potentials, e.g., −0.95 V, hydrogen evolution occurs on the surface, with adsorbed hydrogen on the surface. In Figure 2a, at the open-circuit potential (∼0.3 V), only one broad band at ca. 530 cm^{-1} assigned to Rh−O vibration can be detected and there is no signal from adsorbed pyrazine, which indicates that the Rh surface is mainly covered by oxygen-containing species. With the negative movement of the potential, the signal of rhodium oxides decreases and the signal from pyrazine increases, indicating that the reduction of the surface oxides provides free adsorption sites for pyrazine. The remaining surface oxides will then make the surrounding Rh atom slightly more positively charged due to the strong electronegativity of O, which makes it easier for the pyrazine to bind to the Rh atom with its lone-pair electrons of the N atom. The fact that we observed essentially only those modes related to the in-plane vibration and that no out-of-plane mode was observed leads us to conclude that pyrazine is adsorbed on the surface perpendicularly. However, a slightly tilted configuration along the *Y* direction is also possible because the intensity of the 8b mode increases with decreasing amount of O_{ads} at negative potentials. From SER spectra, we notice that the last vestiges of this broad Rh−O vibration band can only be totally removed at −0.8 V, more negative than the reduction peak between −0.1 and −0.6 V in 1 mM pyrazine + 0.1 M $NaClO_4$ (see the cyclic voltammogram in Figure 1). The reason that only when the potential is moved into the hydrogen evolution region are the surface oxides completely removed could be due to the accelerating effect of adsorbed H on the removal of surface oxides. The adsorbed H will then prevent further tilt of the pyrazine molecule, due to the change in the charge of surface Rh atoms. When the potential is moved back from the negative limit, the desorption of hydrogen provides a surface free of adsorbed H or O for the adsorption of pyrazine. Such an environment facilitates the pyrazine molecule to tilt along the *Y* direction to a more considerable extent, thereby forming the N/π bonded edge-on adsorption configuration that results in a more intense 8b mode than 8a mode. The intensity change reaches the maximum at about −0.5 V, where the amount of H_{ads} is at its minimum while the O is about to adsorb.

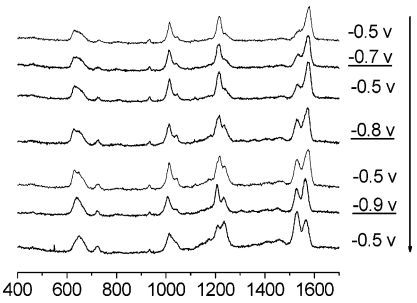

Figure 8. SER spectra of pyrazine adsorbed on a Rh electrode in 1 mM pyrazine + 0.1 M $NaClO_4$ with different negative potential limits. The arrow indicates the potential change sequence.

To confirm the above explanation, we did another experiment in which the negative potential limit was not set in the potential region of hydrogen evolution, but at a less negative value, e.g., −0.7 or −0.8 V, to compare with the −0.9 V case (Figure 8). The arrow in Figure 8 indicates the changing sequence of the potential. As can be seen from the figure, there is only a slight change in the relative intensity of the two bands at ca. 1529 and 1564 cm^{-1} when the potential was stepped to −0.7 or −0.8 V and returned to −0.5 V, with the higher frequency band being stronger. However, if the electrode potential was stepped to −0.9 V (in the hydrogen evolution region) and returned, the relative intensities of the two bands reverse. On the basis of this result, we propose that the adsorbed hydrogen generated from the electrochemical reduction of water may play a key role in the orientation change of pyrazine. It accelerates the complete reduction of rhodium oxides in the hydrogen evolution region and facilitates the coadsorption of pyrazine and hydrogen. On the other hand, if the potential is reversed to a value at which the surface has neither adsorbed hydrogen nor oxygen, pyrazine will behave differently. Under this condition, the orientation change of the adsorbed pyrazine, e.g., from end-on to N/π bonded edge-on, takes place. Furthermore, we find that as long as the potential is reset at some values where large amounts of H or O can be produced, the 8a mode will be stronger than the 8b mode, indicating the end-on adsorption with pyrazine coadsorbing with H or O.

4. Summary

The adsorption behavior of pyrazine on a roughened Rh electrode was studied using surface-enhanced Raman spectros-

copy. The electrode potential and pyrazine concentration effects on the adsorption behavior were examined. The SER spectra of pyrazine on Rh surface show some interesting features involving four pairs of overlapping bands. The relative intensities of the bands in each pair varied significantly with the applied potential, which was not observed on other metals, such as Au, Ag, Cu, Fe, Co, Ni, Ru, and Pd. By analyzing one pair of the overlapping bands and comparing the extent of relative intensity change with different pyrazine concentrations, we proposed that pyrazine orientation change from end-on to N/π bonded edge-on induces the significant relative intensity change of the overlapping bands. Furthermore, the interaction of Rh with hydrogen and oxygen generated at different potentials was proved to have great influence on the pyrazine adsorption configuration. With the coadsorbed hydrogen or oxygen, pyrazine tends to adsorb on the Rh surface through an end-on interaction, but with their removal from the electrode surface, pyrazine will adopt an N/π bonded edge-on configuration. The fact that the SER spectra of pyrazine on Rh show a large difference from those of pyrazine on other metals may be related to a higher affinity of Rh for hydrogen and oxygen.

Acknowledgment. This work is supported by NSFC (20021002, 90206039, 20473067) and MOE of China (20040384010).

References and Notes

(1) Iannelli, A.; Merza, J.; Lipkowski, J. *J. Electroanal. Chem.* **1994**, *376*, 49.
(2) Ikezawa, Y.; Koda, Y.; Shibuya, M.; Terashima, H. *Electrochim. Acta* **2000**, *45*, 2075.
(3) Lazarescu, V. *Surf. Sci.* **1995**, *335*, 227.
(4) Hamm, U. W.; Lazarescu, V.; Kolb, D. M. *J. Chem. Soc., Faraday Trans.* **1996**, *92*, 3785.
(5) Brolo, A. G.; Irish, D. E.; Lipkowski, J. *J. Phys. Chem. B* **1997**, *101*, 3906.
(6) Iannelli, A.; Richer, J.; Lipkowski, J. *Langmuir* **1989**, *5*, 466.
(7) Cai, W. B.; Amano, T.; Osawa. M. *J. Electroanal. Chem.* **2001**, *500*, 147.
(8) Brolo, A. G.; Irish, D. E.; Szymanski, G.; Lipkowski, J. *Langmuir* **1998**, *14*, 517.
(9) Brolo, A. G.; Irish, D. E. *J. Electroanal. Chem.* **1996**, *414*, 183.
(10) Soto, J.; Fernández, D. J.; Centeno, S. P.; López Tocón, I.; Otero, J. C. *Langmuir* **2002**, *18*, 3100.
(11) Conway, B. E.; Dhar, H. P. *Croat. Chem. Acta* **1973**, *45*, 109.
(12) Conway, B. E.; Kozlowska, H. A.; Dhar, H. P. *Electrochim. Acta* 1**974**, *19*, 455.
(13) Conway, B. E.; Mathieson, J. G.; Dhar, H. P. *J. Phys. Chem.* **1974**, *78*, 1226.
(14) Niu, J. J.; Conway, B. E. *J. Electroanal. Chem.* **2004**, *564*, 53.
(15) Otto, A.; Reihl, B. *Surf. Sci.* **1986**, *178*, 635.
(16) Erdheim, G. R.; Birke, R. L.; Lombardi, J. R. *Chem. Phys. Lett.* **1980**, *69*, 495.
(17) Dornhaus, R.; Long, M. B.; Benner, R. E.; Chang, R. K. *Surf. Sci.* **1980**, *93*, 240.
(18) Miranda, M. M.; Neto, N.; Sbrana, G. *J. Phys. Chem.* **1988**, *92*, 954.
(19) Huang, Y.; Wu, G. Z. *Spectrochim. Acta, Part A* **1990**, *46*, 377.
(20) Arenas, J. F.; Woolley, M. S.; Otero, J. C.; Marcos, J. I. *J. Phys. Chem.* **1996**, *100*, 3199.
(21) Tian, Z. Q.; Ren, B.; Wu, D. Y. *J. Phys. Chem. B* **2002**, *106*, 37 and references therein.
(22) Brolo, A. G.; Irish, D. E. *Z. Naturforsch., A* **1995**, *50a*, 274.
(23) Arenas, J. F.; Woolley, M. S.; López Tocón, I.; Otero, J. C.; Marcos, J. I. *J. Chem. Phys.* **2000**, *112*, 7669.
(24) Arenas, J. F.; Soto, J.; López Tocón, I.; Fernández, D. J.; Otero, J. C.; Marcos, J. I. *J. Chem. Phys.* **2002**, *116*, 7207.
(25) Huang, Q. J.; Yao, J. L.; Gu, R. A.; Tian, Z. Q. *Chem. Phys. Lett.* **1997**, *271*, 101.
(26) Huang, Q. J.; Lin, X. F.; Yang, Z. L.; Hu, J. W.; Tian, Z. Q. *J. Electroanal. Chem.* **2004**, *563*, 121.
(27) Ren, B.; Huang, Q. J.; Cai, W. B.; Mao, B. W.; Liu, F. M.; Tian, Z. Q. *J. Electroanal. Chem.* **1996**, *415*, 175.
(28) Cao, P. G.; Yao, J. L.; Ren, B.; Mao, B. W.; Gu, R. A.; Tian, Z. Q. *Chem. Phys. Lett.* **2000**, *316*, 1.
(29) Wu, D. Y.; Xie, Y.; Ren, B.; Yan, J. W.; Mao, B. W.; Tian, Z. Q. *Phys. Chem. Commun.* **2000**, *18*, 1.
(30) Tian, Z. Q.; Ren, B.; Mao, B. W. *J. Phys. Chem. B* **1997**, *101*, 1338.
(31) Tian, Z. Q.; Gao, J. S.; Li, X. Q.; Ren, B.; Huang, Q. J.; Cai, W. B.; Liu, F. M.; Mao, B. W. *J. Raman Spectrosc.* **1998**, *29*, 703.
(32) Cai, W. B.; Ren, B.; Li, X. Q.; She, C. X.; Liu, F. M.; Cai, X. W.; Tian, Z. Q. *Surf. Sci.* **1998**, *406*, 9.
(33) Huang, Q. J.; Li, X. Q.; Yao, J. L.; Ren, B.; Cai, W. B.; Gao, J. S.; Mao, B. W.; Tian, Z. Q. *Surf. Sci.* **1999**, *427/428*, 162.
(34) Tian, Z. Q.; Ren, B.; Chen, Y. X.; Zou, S. Z.; Mao, B. W. *J. Chem. Soc., Faraday Trans.* **1996**, *92*, 3829.
(35) Ren, B.; Lin, X. F.; Yan, J. W.; Mao, B. W.; Tian, Z. Q. *J. Phys. Chem. B* **2003**, *107*, 899.
(36) Chan, H. Y. H.; Zou, S.; Weaver, M. J. *J. Phys. Chem. B* **1999**, *103*, 11141.
(37) Zou, S. Z.; Chan, H. Y. H.; Williams, C. T.; Weaver, M. J. *Langmuir* **2000**, *16*, 754.
(38) Luo, H.; Park, S.; Chan, H. Y. H.; Weaver, M. J. *J. Phys. Chem. B* **2000**, *104*, 8250.
(39) Hallmark, V. M.; Campion, A. *J. Chem. Phys.* **1986**, *84*, 2933.
(40) Vivoni, A.; Birke, R. L.; Foucault, R.; Lombardi, J. R. *J. Phys. Chem. B* **2003**, *107*, 5547.
(41) Birke, R. L.; Lombardi, J. R. In *Spectroelectrochemistry: theory and practice*; Gale, R. J., Ed.; Plenum Press: New York, 1988; pp 263−348.
(42) Haq, S.; King, D. A. *J. Phys. Chem.* **1996**, *100*, 16957.
(43) Wilson, E. B. *Phys. Rev.* **1934**, *45*, 706.
(44) Moskovits, M.; DiLella, D. P.; Maynard, K. J. *Langmuir* **1988**, *4*, 67.